



**Investigation of Non-Thermal Particle Effects  
on Ionization Dynamics in High Current  
Density Ion Beam Transport Experiments**

**H.K. Chung, J.J. MacFarlane, P. Wang, G.A. Moses,  
J.E. Bailey, C.L. Olson, D.R. Welch**

**May 1996  
(revised August 1996)**

**UWFDM-1010**

Presented at the 11th Topical Conference on High-Temperature Plasma Diagnostics,  
Monterey, CA, 12–16 May 1996; to be published in *Review of Scientific Instruments*.

***FUSION TECHNOLOGY INSTITUTE***  
***UNIVERSITY OF WISCONSIN***  
***MADISON WISCONSIN***

### **DISCLAIMER**

This report was prepared as an account of work sponsored by an agency of the United States Government. Neither the United States Government, nor any agency thereof, nor any of their employees, makes any warranty, express or implied, or assumes any legal liability or responsibility for the accuracy, completeness, or usefulness of any information, apparatus, product, or process disclosed, or represents that its use would not infringe privately owned rights. Reference herein to any specific commercial product, process, or service by trade name, trademark, manufacturer, or otherwise, does not necessarily constitute or imply its endorsement, recommendation, or favoring by the United States Government or any agency thereof. The views and opinions of authors expressed herein do not necessarily state or reflect those of the United States Government or any agency thereof.

**Investigation of Non-Thermal Particle Effects on  
Ionization Dynamics in High Current Density  
Ion Beam Transport Experiments**

H. K. Chung, J. J. MacFarlane, P. Wang, and G. A. Moses

Fusion Technology Institute  
Department of Nuclear Engineering and Engineering Physics  
University of Wisconsin-Madison  
Madison, WI 53706

J. E. Bailey, C. L. Olson

Sandia National Laboratories  
Albuquerque, NM, 87185

D. R. Welch

Mission Research Corporation  
Albuquerque, NM, 87106

May 1996  
Revised August 1996

UWFDM-1010

Presented at the 11th Topical Conference on High-Temperature Plasma Diagnostics, Monterey, CA, 12–16 May 1996; to be published in *Review of Scientific Instruments*.

## Abstract

Light ion inertial fusion experiments require the presence of a moderate density background gas in the transport region to provide charge and current neutralization for a high current density ion beam. In this paper, we investigate the effects of non-thermal particles such as beam ions or non-Maxwellian electron distributions on the ionization dynamics of the background gas. In particular, we focus on the case of Li beams being transported in an argon gas. Non-thermal particles as well as thermal electrons are included in time-dependent collisional-radiative calculations to determine time-dependent atomic level populations and charge state distributions in a beam-produced plasma. We also briefly discuss the effects of beam ions and energetic electrons on the visible and VUV spectral regions. It is found that the mean charge state of the gas, and hence the electron density, is significantly increased by collisions with energetic particles. This higher ionization significantly impacts the VUV spectral region, where numerous resonance lines occur. On the other hand, the visible spectrum tends to be less affected because the closely spaced excited states are populated by lower energy thermal electrons.

## 1. Introduction

In light ion beam transport experiments, high energy, high current beam ions ionize a background gas during the transport towards a target. The beam space charge is partly or completely neutralized by the electrons from the gas, and the beam current is partly or completely neutralized by an induced plasma return current.<sup>1</sup> During the breakdown process, energetic electrons are produced from ion impact ionization collisions with gas atoms, knock-on collisions of beam ions with free electrons, and by free electrons being accelerated by electric fields. These non-Maxwellian electrons are predicted to form a hot electron “halo” around the beam, which leads to an increase in plasma conductivity and return current fraction *outside* the beams; this results in higher *net* currents inside the beam channel.<sup>2</sup> It is predicted that the thermalization of these energetic electrons through electron-electron and electron-neutral collisions is sufficiently slow that about 1% of the free electrons reside in a high energy tail. Since the evolution of the plasma conductivity is dependent on the ionization state of the gas, an improved understanding of the physics of ion beam transport can be achieved by studying ionization dynamics, or breakdown physics, of the background gas.

In this paper, we consider the case of Li ion beams incident on an Ar gas. Visible spectra resulting from transitions between excited states of Ar II have been measured in PBFA-II gas cell beam transport experiments.<sup>3</sup> These data have been used to infer the temperature of the relatively cold, “thermal” component of the free electron distribution. The purpose of this current study is to understand the effects of energetic electrons and Li beam ions on the ionization dynamics of these moderate-density Ar plasmas. To do this, we use a time-dependent collisional radiative model which includes collisional excitation and ionization effects due to energetic electrons, Li beam ions, and thermal electrons. The implications for spectroscopic diagnostics are also briefly addressed.

## 2. Theoretical Models

In our time-dependent collisional-radiative (CR) model, ionization and excitation populations are computed by solving multilevel atomic rate equations. The population of each atomic level is determined by computing collisional and radiative transition rates between each level. The ionization and recombination processes considered are: collisional ionization by thermal electrons, Li beam ions and energetic electrons; three-body recombination by thermal electrons; and radiative recombination by thermal and energetic electrons. Three-body recombination by energetic electrons is neglected since energetic particles are less important for the three-body recombination processes.<sup>4</sup> Inner-shell ionization and autoionization processes are included since energetic particles can induce such processes even in a low electron temperature plasma. The excitation and deexcitation processes considered in our calculations are: collisional excitation and deexcitation by thermal and non-thermal electrons, and spontaneous radiative decay. At present, photoexcitation and photoionization are neglected in our calculations. Although photoionization for the Ar gas cell plasmas discussed here should be unimportant, photoexcitation due to resonant self-absorption could lead to lower effective spontaneous decay rates. This will be explored in future calculations.

The rate coefficients for collisional and radiative processes involving thermal electrons and ion beam particles have been described elsewhere.<sup>5,6</sup> The energetic electron collisional excitation and ionization rate coefficients are obtained by integrating collisional cross-sections taken from semi-empirical formulae.<sup>7,8</sup> The form of the energetic electron energy distribution function (which is based on results from particle-in-cell simulations) is assumed to be inversely proportional to electron energy. Particle-in-cell simulations will give a more detailed form of the energetic electron distribution function for our future study. The total number of energetic electrons is taken to be 1% of thermal electrons. The non-thermal electron collisional excitation cross-sections and radiative recombination cross-sections are obtained, respectively, from collisional ionization and photoionization

cross-sections by reciprocity relations.<sup>9</sup> The corresponding rate coefficients are computed by integrating the cross-sections with the energetic electron energy function. In our time-dependent collisional-radiative calculations, 270 atomic levels distributed over 7 ionization stages from Ar I to Ar VII are considered. A configuration averaged atomic model is used in determining populations and charge state distributions. Separate calculations based on a fine-structure atomic model are used to compute spectra. Calculated spectra include contributions from bound-bound, bound-free, and free-free transitions. Opacity effects are included in the spectral calculations. Voigt profiles are used for line profiles.

The plasma and beam conditions used in our calculations are as follows. We assume a constant thermal electron temperature of 3 eV. The 9 MeV Li ion beam current increases linearly with time to 20 kA/cm<sup>2</sup> at 18 ns, and then abruptly falls to zero. The thermal electron density is determined from the effective charge state of the Ar gas, which is updated via the time-dependent collisional-radiative equations. The energetic electron density is assumed to be 1% of the thermal electron density during the beam rise time. The argon gas has a density of  $7 \times 10^{16}$  ions/cm<sup>3</sup> (2 torr at room temperature), and at  $t = 0$  the electron density is assumed to be equal to the ion density.

### 3. Results

First we investigate the effects of energetic particles on collisional rates. The collisional rates considered are an ionization transition from Ar II (singly ionized argon) ground state to Ar III (doubly ionized) ground state, and an excitation transition between Ar II 4p and Ar II 4s (see Figure 1(a) and (b)). The transition between Ar II 4p and Ar II 4s was selected since line emission from transitions of this type have been observed in PBFA-II experiments.

At the low temperatures typical of experimental conditions ( $T \sim 3$  eV), energetic particles provide the dominant source of ionization for large energy transitions. Ionization and excitation due to the energetic electron component exceeds that of the low temperature

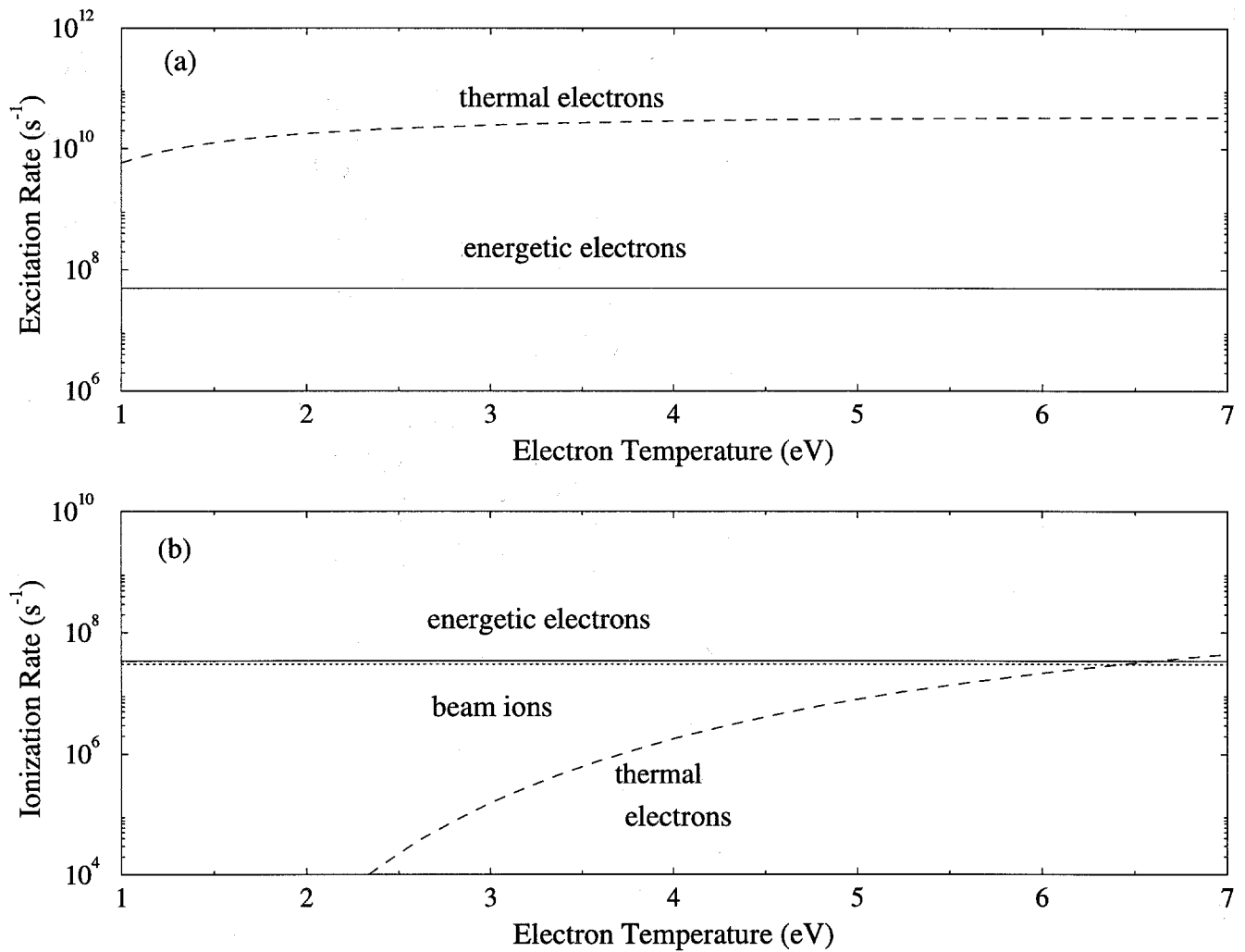


Figure 1. Ionization and excitation rate coefficients for thermal electrons, Li beam ions and energetic electrons plotted as a function of electron temperature: (a) excitation between Ar II 4p and 4s states ( $\Delta E = 2.7$  eV) (b) ionization between Ar II ground state and Ar III ground state ( $\Delta E = 27.7$  eV). Solid line: energetic electron rate. Dotted line: Li beam ion rate. Dashed line: thermal electron rate.



Maxwellian component for  $\Delta E \gtrsim 20$  eV transitions because relatively few particles in the  $T = 3$  eV Maxwellian tail have energies greater than the threshold energy. On the other hand, for small  $\Delta E$  transitions (e.g.,  $4s \rightarrow 4p$ ) a large fraction of the low temperature Maxwellian electrons can participate in the excitation process. Thus, since there are significantly more electrons in the low temperature component of our model, excitation and deexcitation in small  $\Delta E$  transitions (which produce lines in the visible or UV portion of the spectrum) are driven by the thermal electron component.

Due to high excitation and ionization rates for high-energy transitions, beam ions and non-thermal electrons populate high-lying levels. In Figure 2, the population ratio of Ar II 4p to Ar II 4s levels and the ratio of the Ar II ground state to Ar III ground state are shown as a function of time. The population ratios are scaled to their Local Thermodynamic Equilibrium (LTE) values. The LTE population ratios between two levels are based on an electron temperature of 3 eV and an electron density of  $7 \times 10^{16} \text{ cm}^{-3}$ . If the ratio  $f(\text{CR})/f(\text{LTE})$  is unity, the collisional processes are in a detailed balance between the two levels. Figure 2 shows that the relative populations of the two ground states eventually reach a steady-state ratio in which the Ar II is slightly enhanced relative to its LTE value. On the other hand, the relative populations of two excited states, which have a small transition energy, equilibrate very quickly and maintain an LTE ratio. This results from the fact that excitation processes have such a transition energy comparable to or smaller than the electron temperature, and that a detailed balance between collisional processes is established between the two levels in a very short time by thermal electrons. The equilibration time scale for these excited states is  $\sim 10^{-11}$  s.

It should be noted that the energetic particles do not significantly affect the relative populations of the two excited states of a low transition energy.<sup>10</sup> However, the energetic particles do play a significant role in larger  $\Delta E$  transitions. The fact that energetic particles do not cause the relative populations between two closely spaced excited states to deviate significantly from their LTE value has implications for visible spectral measurements. For

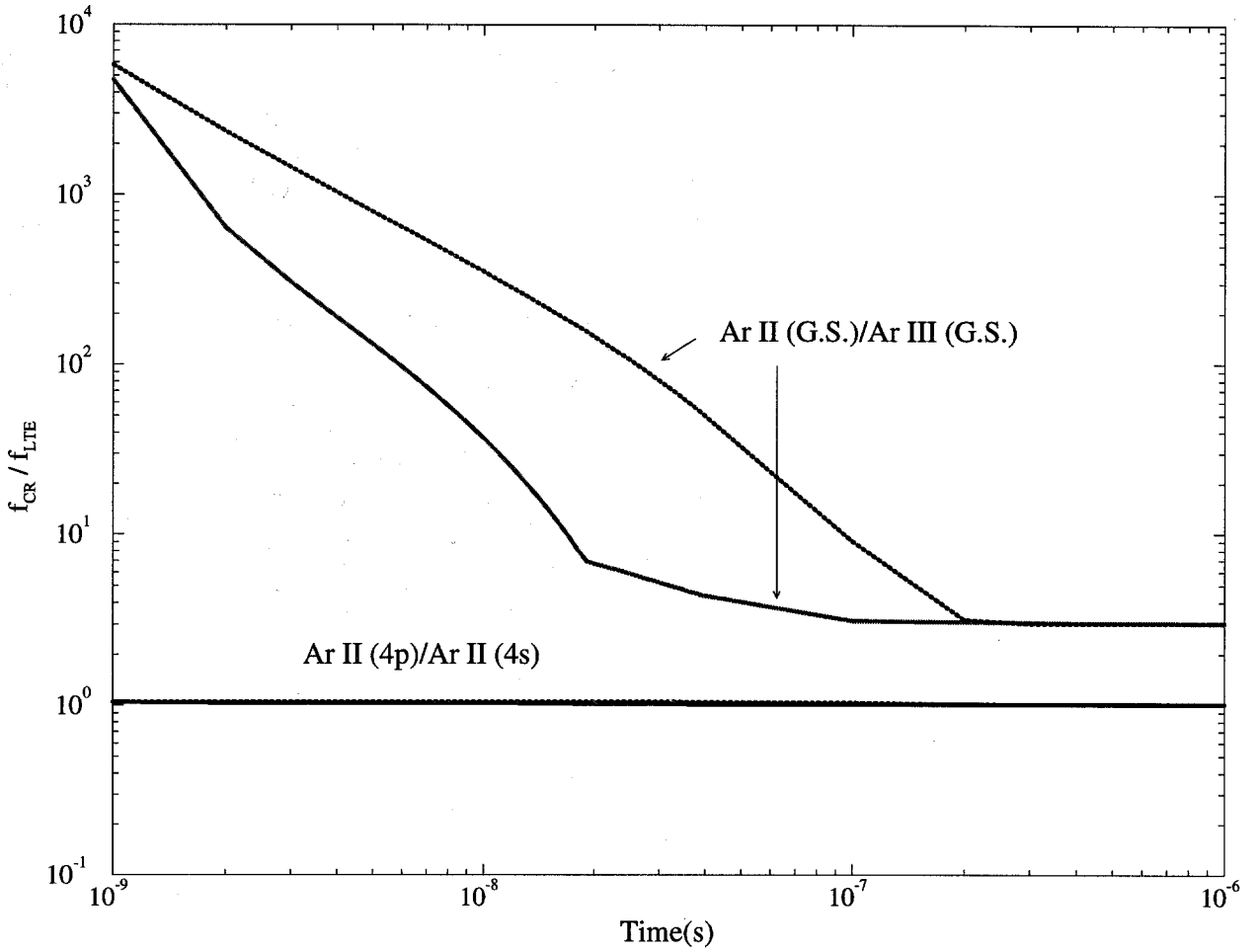


Figure 2. Population ratios for Ar II 4p to 4s ( $\Delta E = 2.7$  eV) and for the Ar II ground state to Ar III ground state ( $\Delta E = 27.7$  eV). Both ratios are scaled to their LTE values. Solid line: the case in which energetic particles are included for the first 18 ns. Dotted line: without energetic particles.

instance, a Boltzmann plot analysis can be used to infer the temperature of the thermal component of the electron distribution.<sup>11</sup>

We next present the results of four simulations which illustrate the effects of energetic particles on the mean charge state of the Ar plasma. Case A refers to a calculation which includes contributions from thermal electrons, Li beam ions, and non-thermal electrons on the Ar ionization dynamics. Case B neglects Li beam ions, but includes thermal and energetic electrons. Case C neglects energetic electrons, but includes thermal electrons and Li beam ions. Case D includes only thermal electrons. For each case, the thermal electron temperature is assumed to be constant at 3 eV and the initial thermal electron density is assumed to correspond to the ion density ( $n_e^{\text{cold}} = 7 \times 10^{16} \text{ cm}^{-3}$ ); that is, all populations are in Ar II ground state at  $t = 0$ . Thus, the calculations provide insight into the processes which affect the growth of the electron density after it has become partially ionized. The Li ion beam and energetic electrons are assumed to rise linearly between  $t = 0$  and 18 ns, and then abruptly fall to zero. Figure 3 shows that the energetic particles can significantly affect the mean charge state. At 18 ns where the Li beam current and non-thermal electron density reach their peak value, the mean charge state for case A differs from the value for case D by a factor of two. For this particular set of plasma and beam conditions, the energetic electrons are seen to be more effective than the Li beam ions in ionizing the singly ionized argon gas. After the energetic particle pulse is removed at 18 ns, the mean charge state for case A stays near its peak value before going into a recombining stage. The mean charge state for case D, however, continues to increase before reaching its steady state value. These results clearly indicate that energetic particle effects play a key role in affecting the ionization dynamics of these moderate-density transport plasmas.

It is of interest to investigate the implications of the above results for spectral diagnostics. Figures 4 and 5 show how energetic particles can affect the visible and VUV spectral region. The visible spectrum results from small  $\Delta E$  transitions is shown and, as

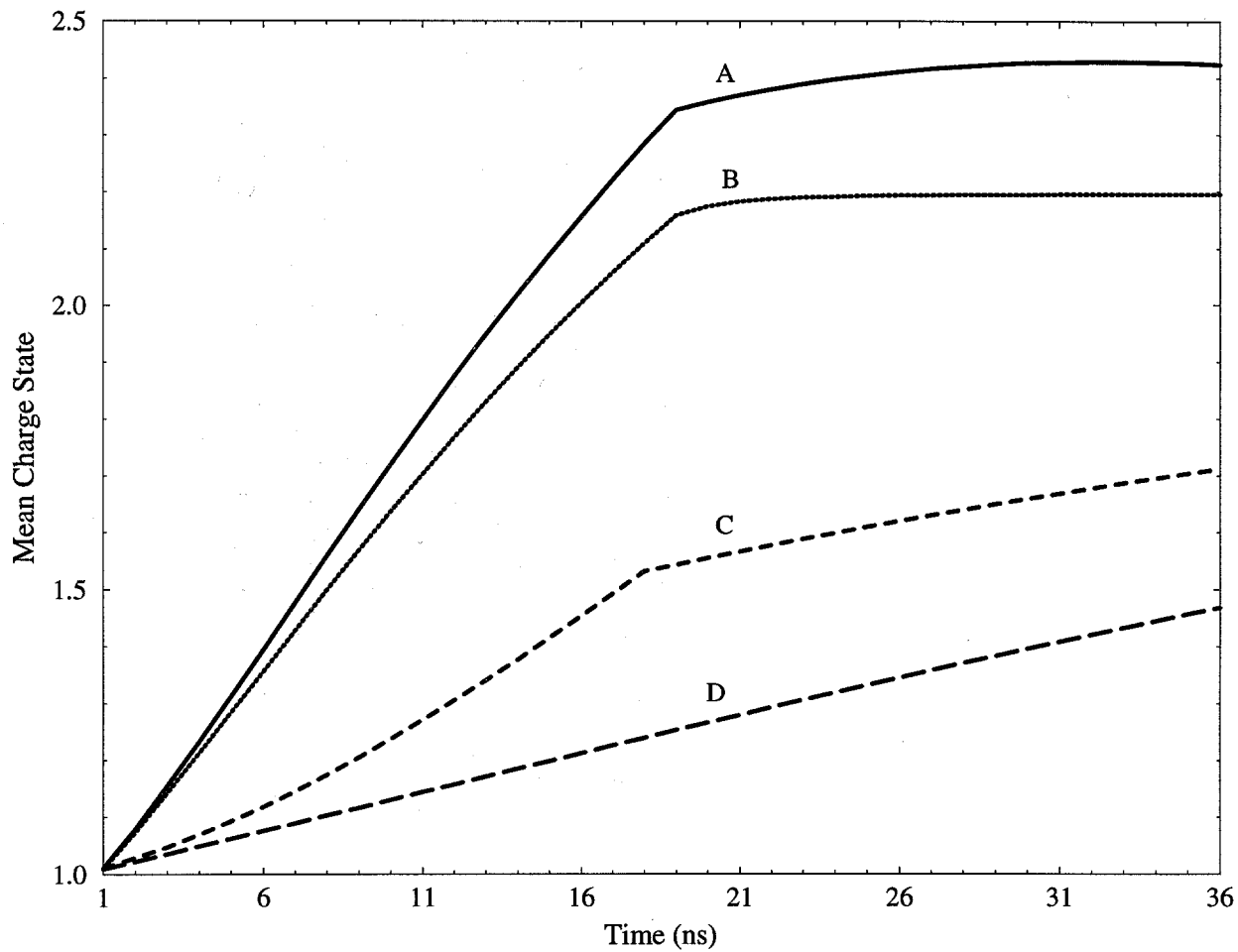


Figure 3. Mean charge state is plotted as a function of time for 4 cases. (A) Includes all energetic particles, Li beam and energetic electrons. (B) Includes energetic electrons but no beam ions. (C) Includes Li beam without energetic electrons. (D) Includes no energetic particles.

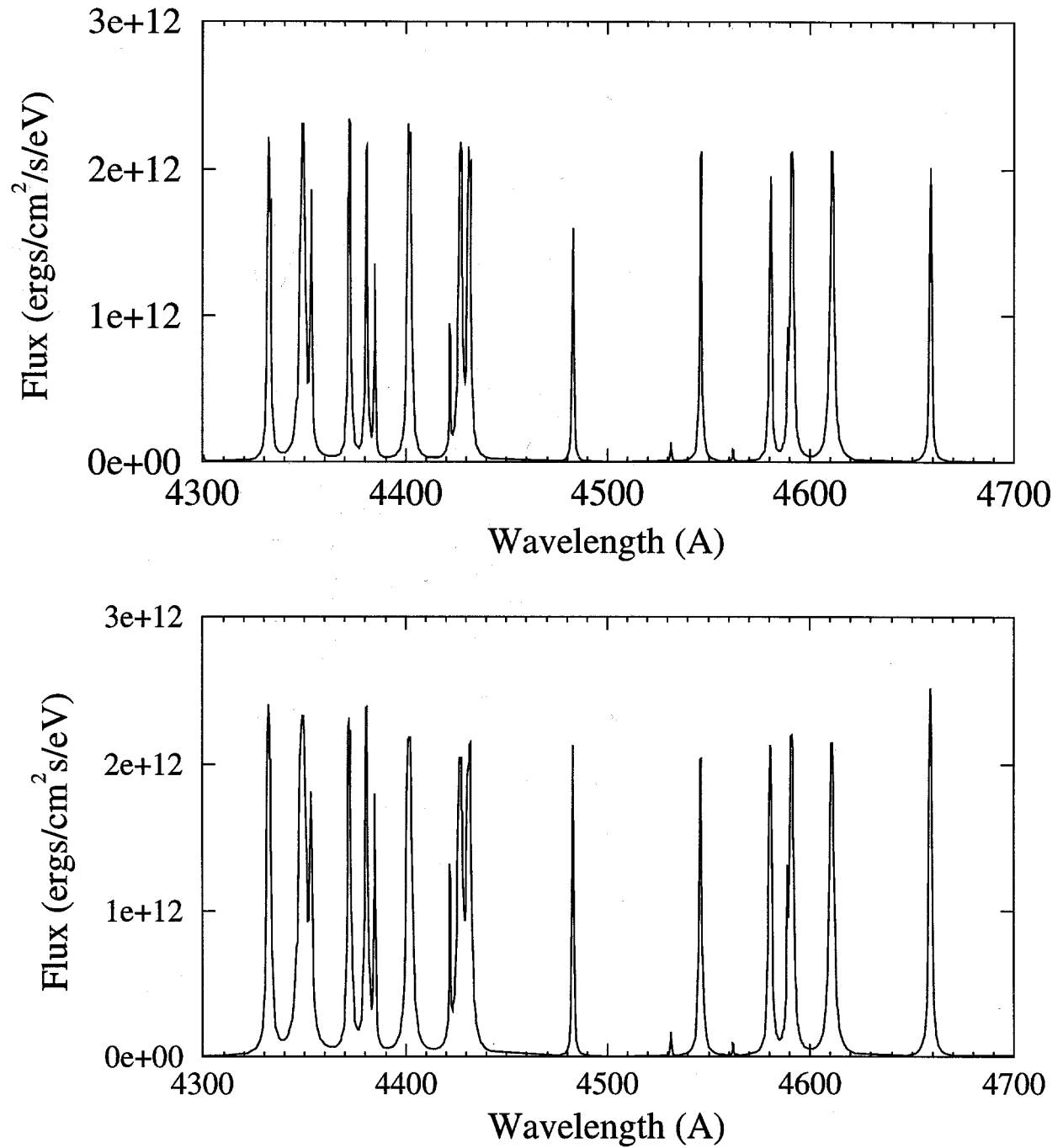


Figure 4. Visible spectra at 18 ns for Case A (top) where energetic particles are included; Case D (bottom) where no energetic particles are included.

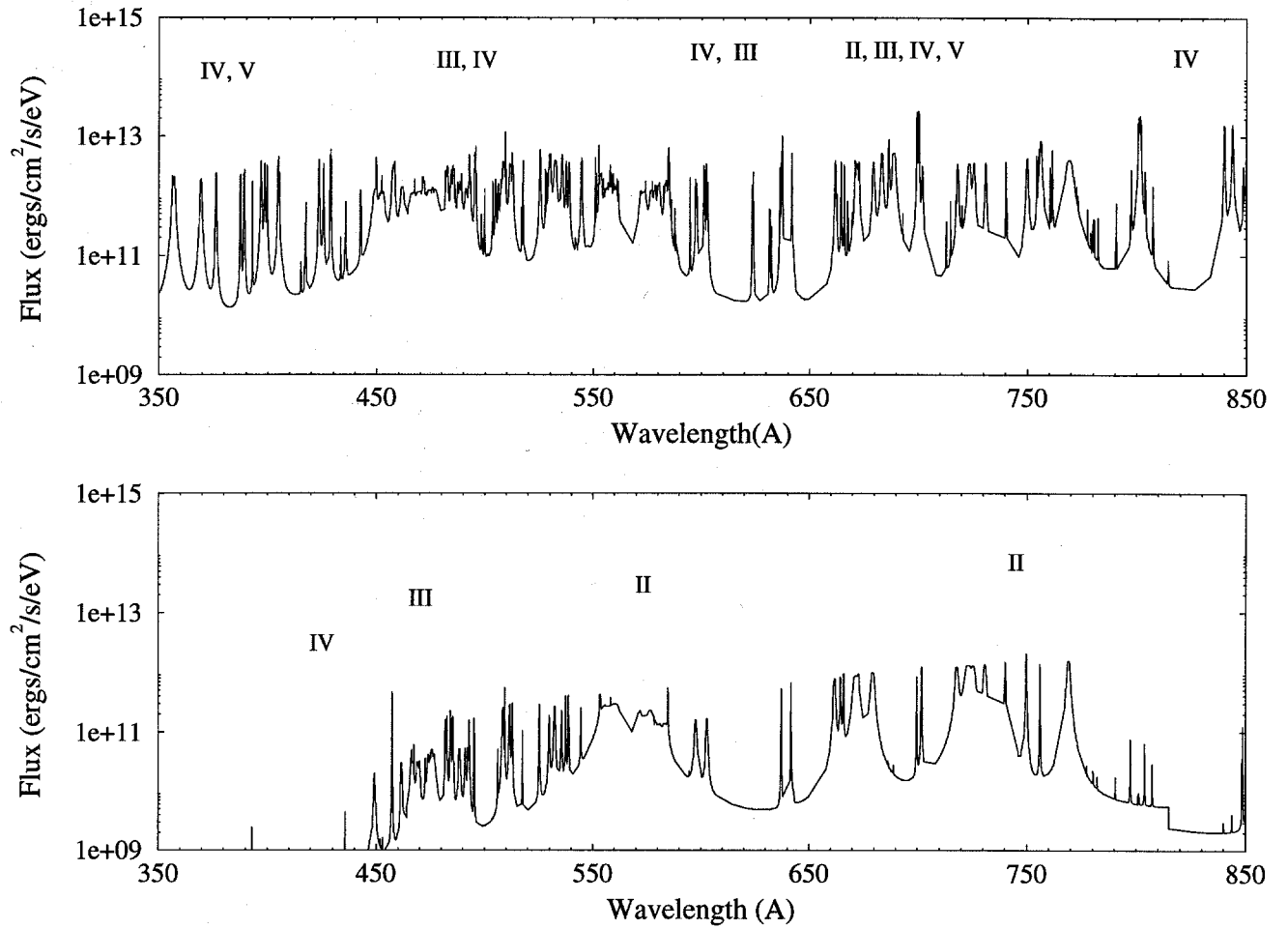


Figure 5. VUV spectral region at 18 ns for Case A (top) and Case D (bottom). Several of the argon lines are identified by their ionization stage.

stated above, is more influenced by thermal electrons. The energetic particles can affect the spectrum in the sense that they influence the absolute population of the excited states, but not their relative populations. Absolute fluxes of many visible lines are close to Planck function-limited values of  $\pi B_\nu$ . This is due to the fact that: (1) the upper and the lower levels of the transition are in LTE with respect to each other; and (2) optical depths for the line cores exceed unity for both cases A and D. It should be noted that if these two conditions are not met, the absolute intensities for the two cases would not necessarily be similar as they are in Figure 4.

In the VUV region, where resonance lines are prominent, the line spectrum can be very significantly affected by energetic particles. Several VUV lines are identified in Figure 5 as coming from high ionization stages such as Ar III, IV or even V when energetic particles are included in the calculation. In simulations which neglect energetic particles, emission lines from the relatively high ionization stages of Ar are not seen. Thus, either emission or absorption spectroscopic measurements could provide valuable information on the ionization dynamics of these transport plasmas. We are also presently investigating whether EUV and x-ray spectral lines resulting from inner-shell transitions can be used to diagnose energetic particle characteristics. This work will be presented elsewhere.

## 4. Summary

Time-dependent collisional-radiative calculations have been performed to investigate the effects of Li beam ions and energetic electrons on the ionization dynamics of light ion beam transport plasmas. We find that energetic particles play a significant role in affecting the ionization dynamics, leading to a higher charge state and a higher electron density in the background plasma. We have also briefly investigated the role of energetic particles in affecting the visible and VUV spectral regions. We find the visible transitions are strongly influenced by thermal electrons, while energetic particles can significantly affect the VUV spectral region.

## Acknowledgement

The work has been supported in part by Sandia National Laboratories.

## References

1. J. A. Swegle and S. A. Slutz, *J. Appl. Phys.* **60**, 3444 (1986).
2. D. R. Welch, C. L. Olson and T. W. L. Sanford, *Phys. Plasmas* **1**, 763 (1994).
3. J. E. Bailey, A. L. Carlson, D. J. Johnson, E. J. McGuire, T. Nash, C. L. Olson, J. J. MacFarlane, and P. Wang, 9th International Conference on High Power Particle Beams, Washington D.C., p. 903 (1992).
4. J. P. Matte, J. C. Kieffer, S. Ethier, M. Chaker, and O. Peyrusse, *Phys. Rev. Lett.* **72**, 1208 (1994).
5. J. J. MacFarlane, P. Wang, J. Bailey, T. A. Mehlhorn, and R. J. Dukart, and R. C. Mancini, *Phys. Rev. E* **47**, 2748 (1993).
6. P. Wang, "ATBASE User's Guide," Univ. of Wisconsin Fusion Technology Institute Report UWFD-942 (December 1993).
7. A. Burgess and H. P. Summers, *Mon. Not. R. Astr. Soc.* **174**, 345 (1976).
8. A. Burgess and M. C. Chidichimo, *Mon. Not. R. Astr. Soc.* **203**, 1269 (1982).
9. I. I. Sobelman, L. S. Vainshtein and E. A. Yukov, *Excitation of Atoms and Broadening of Spectral Lines*, Springer-Verlag, NY (1981).
10. R. Jayakumar and H. H. Fleischmann, *J. Quant. Spectrosc. Radiat. Transfer* **33**, 177 (1985).
11. J. E. Bailey, et al., presented at the Seventh International Workshop on Atomic Physics for Ion-Driven Fusion, Madrid, Spain (October 1995).